A minimalist approach to understanding the efficiency of mononuclear Zn(II) complexes as catalysts of cleavage of an RNA analog†

Ryan A. Mathews, Clifford S. Rossiter, Janet R. Morrow* and John P. Richard*

Received 16th May 2007, Accepted 11th June 2007
First published as an Advance Article on the web 9th July 2007
DOI: 10.1039/b707409c

Mononuclear complexes between Zn^{2+} and the following four macrocycles were prepared: 1,4,7,10-tetraazacyclododecane (**1**), 1-oxa-4,7,10-triazacyclododecane (**2**), 1,5,9-triazacyclododecane (**3**) and 1-hydroxyethyl-1,4,7-triazacyclononane (**4**). The pH rate profiles of values of the observed second-order rate constant log $(k_{Zn})_{app}$ for **Zn(X)(OH$_2$)**-catalyzed cleavage (**X** = **1**, **2**, **3** and **4**) of 2-hydroxypropyl-4-nitrophenyl phosphate (**HpPNP**) show downward breaks centered at the pK_a for ionization of the respective zinc bound water. At low pH, where the rate acceleration for the catalyzed reaction is largest, the stabilizing interaction between the catalyst and the bound transition state is 5.7, 7.4, 7.4 and 5.9 kcal mol^{-1} for the reactions catalyzed by **Zn(1)(OH$_2$)**, **Zn(2)(OH$_2$)**, **Zn(3)(OH$_2$)** and **Zn(4)(OH$_2$)**, respectively. The interactions between the metal cation and the macrocycle cause either a modest increase or reduction in transition state stabilization compared with 6.6 kcal mol^{-1} stabilization for catalysis by **Zn(OH$_2$)$_6$**. The best Zn(II)–macrocycle catalysts are those for which the interactions between the metal ion and macrocycle are the weakest. Inhibition studies show that each of the four catalysts form complexes with phosphate and oxalate dianions with a much higher affinity than diethyl phosphate monoanion, consistent with stronger interaction of the catalysts with the transition state dianion compared with the substrate monoanion **HpPNP**. The pH-dependence of methyl phosphate inhibition of **Zn(2)** catalyzed cleavage of **HpPNP** shows that only the **Zn(2)(OH$_2$)** species binds the inhibitor. This result is consistent with a mechanism that has **Zn(2)(OH$_2$)** as the active catalytic species.

Introduction

The development of effective small molecule catalysts of the cleavage of RNA is a problem that will be solved largely through synthetic design, while the mechanism of action and catalytic efficiency of existing small molecule catalysts will be determined mainly through the physical characterization of the catalyst and of its kinetic mechanism of action. The second kind of studies provide fundamental information about mechanism that may lead to the insight needed to identify target molecules of high catalytic activity.[1–7]

We are interested in understanding the origin of the rate accelerations observed for catalysis of phosphate diester cleavage by small macrocycle complexes of Zn(II).[3,8–11] Macrocycles with several basic nitrogen atoms act to encapsulate the Zn(II) cation in water.[12–15] It is known that hydrated Zn(II) catalyzes hydrolysis of RNA-analogs.[16,17] However, the catalysis is limited by the low solubility of Zn(II) in aqueous solution at neutral pH and the fall-off in solubility as the pH is increased above 7.[18,19] Therefore, an important function of the macrocyclic ring is to *draw* the metal cation into basic aqueous solution, where it may act as a catalytic center. In this paper we consider the question of whether these macrocycles act mainly to keep Zn(II) in a form that is soluble in basic solution where phosphate diesters show an intrinsically high reactivity toward cleavage,[20] or, if Zn(II) is also activated by complex formation, to catalyze the cleavage reaction.

The activity of hydrated Zn(II) towards catalysis of cleavage of the simple RNA analog 2-hydroxypropyl 4-nitrophenyl phosphate (**HpPNP**) provides a point of reference for examining the effect of macrocycle ligands on catalytic activity. We report here the results of a comprehensive examination of the effect of four macrocycles, **Zn(1)–Zn(4)** (Scheme 1), on the stabilization of the transition state for cleavage of **HpPNP** relative to the stabilization observed for catalysis by free Zn^{2+}. Our data show that some ligands have the effect of increasing the transition-state stabilization at pH 7 by 0.8 kcal mol^{-1} compared with that observed for free Zn^{2+}, while

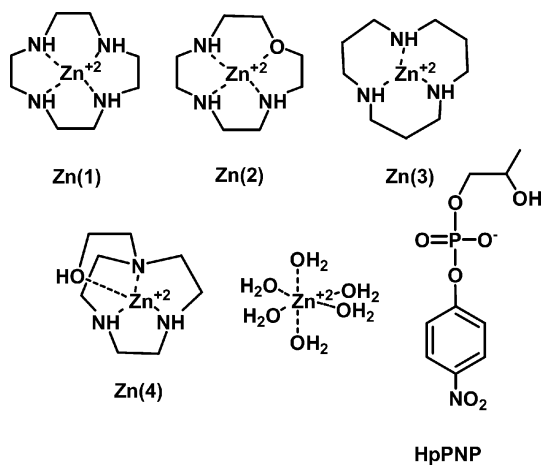

Scheme 1

Department of Chemistry, University at Buffalo, SUNY, Buffalo, NY 14260, USA. E-mail: jmorrow@buffalo.edu, jrichard@buffalo.edu

† Electronic supplementary information (ESI) available: Table S1 and Fig. S1–S2. See DOI: 10.1039/b707409c

other ligands decrease this transition state stabilization by up to 0.9 kcal mol^{-1}, but that these ligand effects are small compared with the 6.6 kcal mol^{-1} stabilization observed for catalysis by **Zn(OH$_2$)$_6$**.

We have examined the macrocyclic ligand effects on several other coordination properties of these Zn^{2+}-complexes. Our results are consistent with the notion that the catalytic activity of **Zn(1)–Zn(4)** towards cleavage of **HpPNP** is due mainly to stabilization of the reaction transition state by electrostatic interactions between the metal dication and the transition-state dianion but that there are smaller second-order effects of these ligands on activity which are difficult to fully rationalize. Our studies demonstrate the relationship between anion coordination and Zn(II) catalysis and provide a guideline for the design of more effective catalysts. In the analysis here, **Zn(X)** denotes all species that contain Zn(II) bound to macrocycle **X**. Water or hydroxide ligands are specified as needed, for example **Zn(X)(OH$_2$)** or **Zn(X)(OH$^-$)**.

Results

Potentiometric titrations of solutions that contain 1.00 mM macrocycles **1** or **2** and 1.00 mM $Zn(NO_3)_2$ at 25 °C and I = 0.10 M ($NaNO_3$) show two inflection points (See ESI†, Fig. S1 and S2). The broad inflection point at low pH is due to the release of protons from the macrocycle upon binding of Zn(II). The second inflection point arises from loss of a proton from a group with a pK_a of 7.8 or 7.7 (Table 1). We assign the second inflection to the ionization of a Zn(II)-bound water to form a Zn(II)-bound hydroxide. The fits of these data to a standard scheme gave the values of K_{Mac} for formation of **Zn(1)(OH$_2$)** and **Zn(2)(OH$_2$)** from Zn^{2+} and the respective ligand, and the pK_a for ionization of the zinc-bound water (Table 1). Literature values for pK_a and K_{mac} for **Zn(3)(OH$_2$)** and **Zn(4)(OH$_2$)** are also reported in Table 1.

The cyclic phosphate diester was identified by ^{31}P NMR as the sole phosphorus-containing product of cleavage of **HpPNP** catalyzed by the Zn(II) complexes examined in this work. The ligands **1–4** all bind Zn(II) with high affinity (Table 1): ≥ 99% of free Zn(II) is converted to the macrocycle complex in solutions at pH 7.6 when $[Zn(II)]_T$ = 1.0 mM and there is a 5% excess of **1**, **2**, or **4**. The ligand **3** binds to Zn(II) most weakly, and 5% of free Zn(II) is present at pH 7.6 when $[Zn(II)]_T$ = 1.0 mM. The second-order rate constants for cleavage of **HpPNP** catalyzed by **Zn(1)(OH$_2$)** -**Zn(4)(OH$_2$)**, $(k_{Zn})_{app}$, were determined as the slopes of linear correlations of k_{obsd} against the concentration of the metal ion complex (0.2–4.0 mM). The second-order rate constant for cleavage of **HpPNP** catalyzed by **Zn(3)(OH$_2$)** at pH 7.6 was obtained using observed rate constants determined for reactions catalyzed by 1.0–4.0 mM **Zn(3)(OH$_2$)**.

The solid symbols in Fig. 1 show the pH rate profiles of values of $(k_{Zn})_{app}$ for catalysis of the cleavage of **HpPNP** by **Zn(1)(OH$_2$)–Zn(4)(OH$_2$)**. The solid lines in Fig. 1 are the theoretical fits of the experimental data to eqn (1) derived for Scheme 2 for a reaction that is controlled by the ionization of a zinc-bound water. The values of the parameters k_{Zn} (M^{-1} s^{-1}) and K_a (M) determined by this fitting procedure are reported in Table 1. There

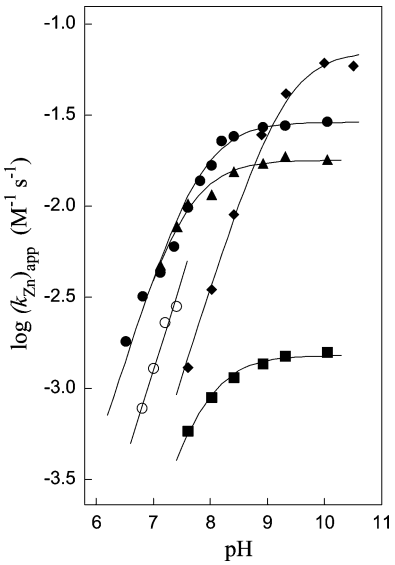

Fig. 1 pH rate profiles of second-order rate constants $(k_{Zn})_{app}$ for cleavage of **HpPNP** catalyzed by several mononuclear Zn(II) complexes. Key: **Zn(1)**, (■); **Zn(2)**, (●); **Zn(3)**, (▲); **Zn(4)**, (♦); **Zn(OH$_2$)$_6$**, (○). The solid lines through values for $(k_{Zn})_{app}$ show the theoretical fits of these data to eqn (1) derived for Scheme 2.

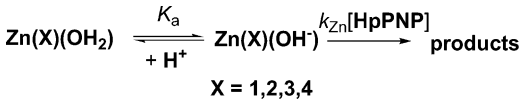

Scheme 2

Table 1 Kinetic parameters, binding and ionization constants for catalysis of cleavage of **HpPNP** by **Zn(OH$_2$)$_6$** and by Zn(II) macrocycle complexes at 25 °C and I = 0.10 ($NaNO_3$)

Catalyst	K_{Mac} [a]	k_{Zn}/$M^{-1}s^{-1}$ [b]	pK_a [c]	$k_{Zn}K_a/K_w$ $M^{-2}s^{-1}$ [d]	k_{rel} [e]
Zn(H$_2$O)$_6$		3×10^{-1}	(9.5)	6.7×10^{3}	1
Zn(1)(OH$_2$)	2×10^{15}	1.5×10^{-3}	7.8 (7.8)	1.5×10^{3}	0.22
Zn(2)(OH$_2$)	5×10^{10}	2.8×10^{-2}	7.8 (7.7)	2.7×10^{4}	4.0
Zn(3)(OH$_2$)	6×10^{8} [f]	1.8×10^{-2}	7.6 (7.5)[g]	2.8×10^{4}	4.2
Zn(4)(OH$_2$)	4×10^{11} [g]	7.2×10^{-2}	9.3 (9.2)[g]	2.2×10^{3}	0.33

[a] The equilibrium constant for the combination of **X** in neutral form and Zn(II) to form **Zn(X)(OH$_2$)**. [b] The limiting second-order rate constant for **Zn(X)(OH$_2$)**-catalyzed cleavage of **HpPNP** determined at high pH (Fig. 1). The value for **Zn(OH$_2$)$_6$** was obtained from the third-order rate constant in column 5 and pK_a of 9.5. [c] The pK_a for ionization of the Zn(II)-bound water determined from the fits of the plots shown in Fig. 1 to eqn (1). The values in parentheses were determined by potentiometric titration and the pK_a for **Zn(OH$_2$)$_6$** is from the literature.[18, 21] [d] Third-order rate constant for cleavage of **HpPNP** by **Zn(X)(OH$_2$)** at pH ≪ pK_a (Scheme 5) calculated by using the data in Fig. 1 and eqn (1) ($[H^+] \gg K_a$ and $[H^+] = K_w/[HO^-]$). For **Zn(OH$_2$)$_6$**, a third-order rate constant was determined from a plot of the second-order rate constant $(k_{Zn})_{app}$ as a function of $[OH^-]$ concentration. [e] Relative value of the third-order rate constant for **Zn(X)** complexes relative to that of **Zn(OH$_2$)$_6$**. [f] Literature value.[22] [g] Literature value.[3]

is good agreement between the values of K_a determined by pH–potentiometric titration and by fitting the kinetic data. The open symbols in Fig. 1 show data for catalysis of the cleavage of **HpPNP** by free **Zn(OH$_2$)$_6$**. It was not possible to obtain kinetic data at pH = pK_a = 9.5 for the zinc-bound water, because of the low solubility of Zn(II) at high pH.

$$(k_{Zn})_{app} = \left[\frac{k_{Zn}K_a}{K_a + [H^+]}\right] \quad (1)$$

Fig. 2A shows the decrease in the normalized rate constants k_{obsd}/k_o for the cleavage of **HpPNP** catalyzed by 1.0 mM **Zn(X)(OH$_2$)** for reactions in the presence of increasing concentrations of methylphosphate dianion (**CH$_3$OPO$_3^{2-}$**), where k_{obsd} (s^{-1}) is the observed first-order rate constant for the cleavage reaction, and k_o (s^{-1}) is the observed rate constant when [**CH$_3$OPO$_3^{2-}$**] = 0. These data were fit to Scheme 3, which shows **CH$_3$OPO$_3^{2-}$** and substrate competing for binding to the catalyst. The binding of methylphosphate is so tight that very little catalytic activity is observed when [**CH$_3$OPO$_3^{2-}$**] > 10 [**Zn(X)(OH$_2$)**] = 1.0 mM. Therefore, it was not possible to work with inhibitor concentrations that are in great excess of the catalyst concentration and make the usual assumption in fitting these data to Scheme 3 that formation of **Zn(X)(CH$_3$OPO$_3^{2-}$)** does not significantly affect concentration of the unbound inhibitor. The solid lines in Fig. 2A show the least squares fit of data to eqn (2) derived for Scheme 3 where $[L]_T$ is total Zn(II) complex concentration, $[I]_T$ is the total inhibitor concentration and $(K_i)_{obs}$ is the inhibition constant at a given pH. The values of K_i determined by this fitting procedure are reported in Table 2. Fig. 2B shows the decrease in the normalized rate constants k_{obsd}/k_o for the cleavage of **HpPNP** catalyzed by 1.0 mM **Zn(X)(OH$_2$)** as the concentrations of oxalate dianion (**C$_2$O$_4^{2-}$**) is increased.

$$\frac{k_{obsd}}{k_o} = \frac{[L]_T - [I]_T - (K_i)_{obsd} + \sqrt{[L]_T^2 + [I]_T^2 + (K_i)_{obsd}^2 - 2[L]_T[I]_T + 2[L]_T(K_i)_{obsd} + 2[I]_T(K_i)_{obsd}}}{2[L]_T} \quad (2)$$

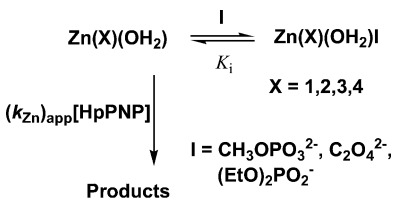

Scheme 3

There is only weak inhibition by diethyl phosphate of the cleavage of **HpPNP** catalyzed by **Zn(X)**. This inhibition was evaluated by fitting plots of k_{obsd}/k_o against inhibitor concentration (Fig. 3) to eqn (3). This equation was derived for Scheme 3 by making the simplifying assumption that formation of the complex between inhibitor and **Zn(X)** does not cause a significant change in the concentration of free inhibitor in solution. The inhibition constants K_i determined from these data are reported in Table 2.

$$\frac{k_{obs}}{k_o} = \left[\frac{(k_{Zn})_{app}[Zn(X)]}{1 + \frac{[DEP]}{(K_i)_{obs}}}\right]\frac{1}{k_o} \quad (3)$$

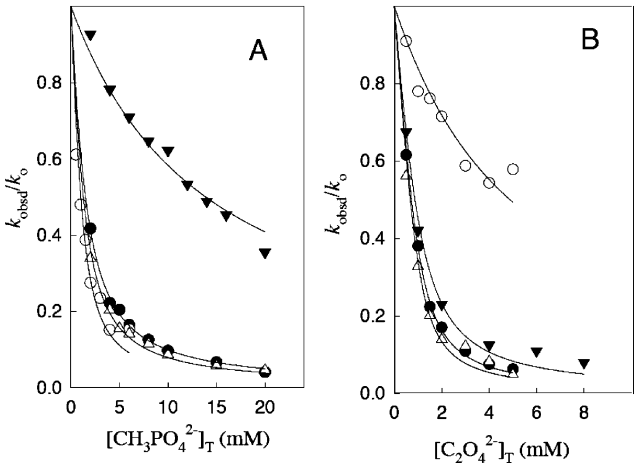

Fig. 2 The effect of increasing total concentration of inhibitor dianion on the normalized rate constant k_{obsd}/k_o for cleavage of **HpPNP** catalyzed by [**Zn(X)(OH$_2$)**] = $[L]_T$ = 1.0 mM and pH = 7.6 as fit to eqn (2). Fig. 2A—Inhibition by methylphosphate dianion. Key: **Zn(1)**, (○); **Zn(2)**, (●); **Zn(3)**, (△); **Zn(4)**, (▼). Fig. 2B—Inhibition by oxalate dianion. Key: **Zn(1)**, (○); **Zn(2)**, (●); **Zn(3)**, (△); **Zn(4)**, (▼).

Table 2 Inhibition constants K_i for formation of complexes between Zn(X)(OH$_2$) and simple monoanions and dianions.[a]

K_i (mM)[b] or ($-\Delta G_A$ (kcal mol^{-1}))			
Complex	Diethyl-phosphate	Methyl-phosphate	Oxalate
Zn(1)	46 (1.8)	0.51 (4.5)	4.4 (3.2)
Zn(2)	42 (1.9)	1.0 (4.1)	0.23 (5.0)
Zn(3)	29 (2.1)	0.78 (4.2)	0.18 (5.1)
Zn(4)	94 (1.4)	13 (2.6)	0.37 (4.7)

[a] For reactions at constant ionic strength of I = 0.10 M (NaNO$_3$) at pH = 7.6 and 25 °C. [b] Value of K_i determined from the non linear least squares fit of the plots shown in Fig. 2 and 3 to the kinetic eqn (2) or (3), respectively.

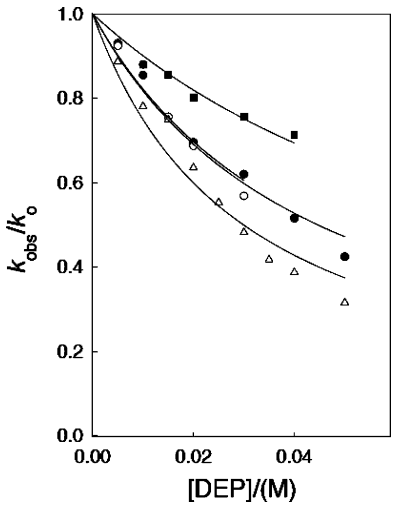

Fig. 3 The effect of increasing total concentration of added diethyl phosphate (**DEP = PO$_2$(OEt)$_2^-$**) monoanion on the normalized rate constant k_{obsd}/k_o for cleavage of **HpPNP** catalyzed by [**Zn(X)(OH$_2$)**] = $[L]_T$ = 1.0 mM. Data was fit to eqn (3). Key: **Zn(1)**, (○); **Zn(2)**, (●); **Zn(3)**, (△); **Zn(4)**, (■).

Table S1 of the ESI† reports the values of $(K_i)_{obsd}$ determined for inhibition of **Zn(2)(OH$_2$)**-catalyzed cleavage of **HpPNP** by methylphosphate dianion at pH 7.6–10. Representative data for the reaction at pH 7.6 are shown in Fig. 2A. The values of $(K_i)_{obsd}$ for inhibition at higher pH were obtained from similar plots of k_{obsd}/k_o against $[\mathbf{MeOPO_3}^{2-}]_T$. Fig. 4 shows the plot of $(K_i)_{obsd}$ for inhibition of **Zn(2)(OH$_2$)**-catalyzed cleavage of **HpPNP** by methylphosphate against the reaction pH. The solid line for Fig. 4 shows the least-squares fit of the data to eqn (4), with $K_a = 10^{-7.8}$ M (Table 1) and $K_i = 0.4$ mM for inhibition at low pH, where the catalyst is fully protonated.

$$(K_i)_{obsd} = \left(\frac{K_i(K_a + [H^+])}{[H^+]}\right) \quad (4)$$

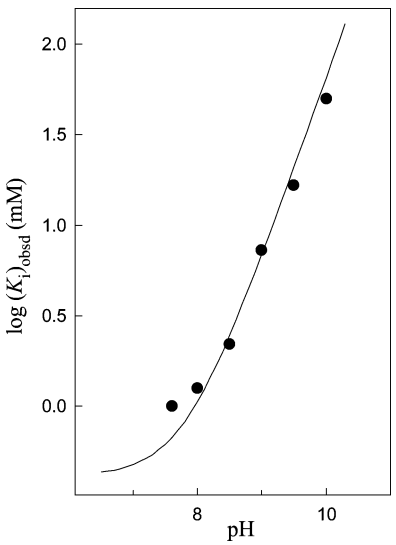

Fig. 4 The pH profile of values of $(K_i)_{obsd}$ for inhibition of **Zn(2)(OH$_2$)**-catalyzed transesterification of **HpPNP** by methylphosphate dianion (**CH$_3$OPO$_3^{2-}$**) fit to eqn (4).

Discussion

The following close parallels between the experimental results presented here for catalysis of cleavage of **HpPNP** by mononuclear complexes and results obtained for catalysis by the dinuclear catalyst **Zn$_2$(5)** (Scheme 4) show that these catalysts follow similar reaction mechanisms (Schemes 5 and 6).[3, 10]

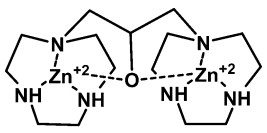

Zn$_2$(5)

Scheme 4

(1) The pH rate profiles of second-order rate constants $(k_{Zn})_{app}$ for both the mono and dinuclear catalysts show downward breaks at the pK_a for loss of a proton from a zinc-bound water. This shows that the Zn(II) catalyst substrate complex is converted to the active form by loss of a proton. Two kinetically equivalent pathways (Scheme 5) that give this pH-profile are: (a) **Zn(2)(OH$^-$)** catalyst

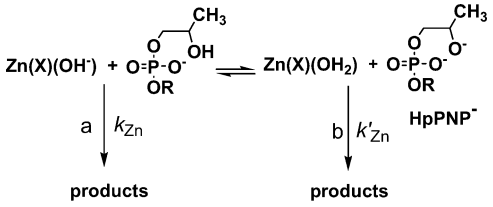

Scheme 5

interaction with the neutral **HpPNP** substrate to deprotonate the 2′-hydroxyl or (b) interaction of the deprotonated substrate (**HpPNP**$^-$) with the **Zn(2)(OH$_2$)** catalyst. Pathway b is strongly supported by the absence of a primary solvent deuterium isotope effect on the cleavage of uridine 3′,4-nitrophenyl phosphate (**UpPNP**) catalyzed by **Zn$_2$(5)(OH$_2$)**.[10] Further studies here on the pH dependence of methylphosphate inhibitor binding are also supportive of pathway b as discussed further below.

(2) The cleavage of **HpPNP** catalyzed by the mononuclear catalysts and by the dinuclear catalyst **Zn$_2$(5)** are both inhibited by methyl phosphate dianion[23] and diethyl phosphate monoanion.[3] The dinuclear complex is both a better catalyst than the mononuclear complexes, and is more strongly inhibited by both methyl phosphate dianion and diethyl phosphate monoanion. Furthermore, the dinuclear catalyst shows a 1600-fold greater selectivity for binding the dianion compared with the monoanion, while the mononuclear catalysts shows at most a 100-fold selectivity for dianion binding. These observations are consistent with the conclusion that the stabilizing interactions between the catalyst and inhibitor are largely electrostatic and are stronger for the more highly charged dinuclear catalyst.

(3) The values of $(K_i)_{obsd}$ for inhibition of **Zn(2)(OH$_2$)**-catalyzed cleavage of **HpPNP** by methylphosphate dianion decrease by 50-fold as the pH is decreased from 10–7.6 (Fig. 4). These data show that the inhibitor is specific for binding to the aqua complex **Zn(2)(OH$_2$)** and does not bind tightly to the ionized complex Zn(**2**)(**OH**$^-$). A similar pH dependence has been observed for the values of K_i for methylphosphate inhibition of the dinuclear complex **Zn$_2$(5)**-catalyzed cleavage of **HpPNP**.[23]

Note the small difference between the value of $(K_i)_{obsd} = 1.0$ mM for inhibition of **Zn(2)(OH$_2$)**-catalyzed cleavage of **HpPNP** at pH 7.6 (Table 2) and $K_i = 0.4$ mM estimated for the reaction at low pH where all of the complex is present in the high-affinity, protonated form. The values of $(K_i)_{obsd}$ determined at pH 7.6 (Table 2) and K_i as defined by Scheme 6 are also expected to differ slightly for other **Zn(X)(OH$_2$)**-catalyzed reactions. However, this should not have a large effect on the relative values of $(K_i)_{obsd}$

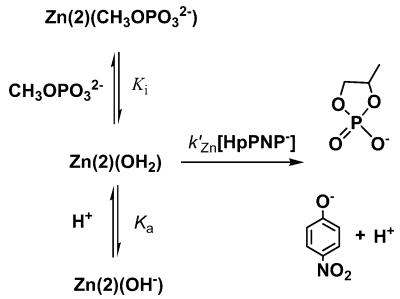

Scheme 6

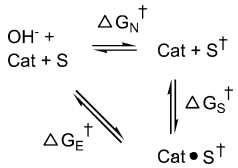

Scheme 7

determined for the reactions catalyzed by different macrocycle complexes **Zn(X)(OH$_2$)**, because each of these complexes exists largely in the high affinity protonated form at pH 7.6.

The break in the pH profile in Fig. 4 at pH = pK_a = 7.8 for ionization of **Zn(2)(OH$_2$)** to form **Zn(2)(OH$^-$)** provides compelling support for a mechanism in which **Zn(2)(OH$_2$)** is the active form of catalyst that is selective for binding and catalysis of the reaction of 2′-hydroxyl ionized substrate **HpPNP$^-$** (Schemes 5 and 6).[10] The active catalyst **Zn(2)(OH$_2$)** shows strong affinity for binding to the methyl phosphate dianion and this binding affinity falls off with deprotonation of the catalyst to form **Zn(1)(OH$^-$)**. The concentration of **HpPNP$^-$** increases as the pH is increased from 7–10. The values of $(k_{Zn})_{app}$ (Fig. 1) reflect this increase so long as the concentration of the active catalysts **Zn(X)(OH$_2$)** remains constant, but $(k_{Zn})_{app}$ reaches a limiting value at high pH where there are compensating increases and decreases in the concentration of **HpPNP$^-$** and **Zn(2)(OH$_2$)**, respectively.

Catalytic efficiency

The relative catalytic efficiencies of **Zn(X)(OH$_2$)** for reactions at low pH,[11] where the catalysts exist mainly in the active aqua form, is related to the position of the lines of slope in Fig. 1. These lines are defined by the apparent third order rate constants $k_{zn}k_a/k_w$ for the **Zn(X)(OH$_2$)**-catalyzed reactions at low pH. The values for these composite rate constants were calculated for the **Zn(X)(OH$_2$)**-catalyzed reaction using the data in Fig. 1 and eqn (1) (with $[H^+] \gg K_a$ and $[H^+] = K_w/[HO^-]$). For **Zn(OH$_2$)$_6$**, a third-order rate constant was determined from a plot of the second-order rate constant $(k_{Zn})_{app}$ for different concentrations of hydroxide ion.

$$\Delta G_{S\dagger} = \Delta G^{\dagger}_{E} - \Delta G^{\dagger}_{N} = -RT \ln \left[\frac{k_{ZN} K_a / K_w}{k_{HO}} \right] \qquad (5)$$

The total stabilization of the transition state for the reactions at low pH by interaction with Zn^{2+}-catalysts can be calculated from the ratio of the apparent third-order rate constant for the catalyzed reaction, $k_{zn}k_a/k_w$, and k_{HO} for hydroxide-ion catalyzed cleavage of **HpPNP**, using eqn (5) derived for Scheme 7.[8] The ratio of the rate constant for the catalyzed reaction to the rate constant for the background reaction is used to estimate the transition state stabilization which can formerly be considered as the free energy of binding of the catalyst (cat) to transition state (S†).[24] Substitution[8] into eqn (5) of k_{HO} = 0.099 M^{-1} s^{-1} and $k_{zn}k_a/k_w$ = 6.7 × 10^3 M^{-2} s^{-1} for the reaction catalyzed by **Zn(OH$_2$)$_6$** gives a 6.6 kcal mol^{-1} transition state stabilization ($\Delta G_{S\dagger}$) from interaction between the metal cation and the oxyphosphorane like transition state. Values of $\Delta G_{S\dagger}$ for **Zn(1)(OH$_2$)**, **Zn(2)(OH$_2$)**, **Zn(3)(OH$_2$)** and **Zn(4)(OH$_2$)** are 5.7, 7.4, 7.4 and 5.9 kcal mol^{-1}, respectively.

The catalytic activity for **Zn(X)(OH$_2$)** may also be defined as the limiting second-order rate constant k_{Zn} observed at high pH, where most of the catalyst has undergone ionization to form inactive **Zn(X)(OH$^-$)**. This limiting rate constant depends both upon the intrinsic catalytic activity of **Zn(X)(OH$_2$)** ($k_{zn}k_a/k_w$) and the pK_a of the zinc-bound water. For example, **Zn(4)(OH$_2$)** shows a low catalytic reactivity relative to other catalysts at low pH (Fig. 1), and a much higher relative activity at pH 10 because the high pK_a for **Zn(4)(OH$_2$)** allows large concentrations of the active catalyst to exist at high pH where there is a large concentration of the reactive ionized substrate form **HpPNP$^-$**. At pH values close to physiological pH (7.6), **Zn(2)** and **Zn(3)** are the most effective catalysts ($(k_{Zn})_{app}$ = 1.0 × 10^{-2} M^{-1} s^{-1} for both) whereas **Zn(1)** and **Zn(4)** are the least effective ($(k_{Zn})_{app}$ = 5.8 × 10^{-4} and 1.3 × 10^{-3} M^{-1} s^{-1}, respectively).

Table 1 compares the catalytic activity of mononuclear catalysts **Zn(X)(OH$_2$)** to the activity of **Zn(OH$_2$)$_6$**. The apparent third-order rate constant $k_{zn}k_a/k_w$ for the reaction catalyzed by **Zn(OH$_2$)$_6$** lies midway between the rate constant for the most and least reactive **Zn(X)(OH$_2$)** complexes. The most reactive and unreactive **Zn(X)(OH$_2$)** provide a 0.8 kcal mol^{-1} stabilization and a 0.9 kcal mol^{-1} destabilization, respectively, of the transition state for cleavage of **HpPNP**.[25] These ligand effects are small compared with the 6.6 kcal mol^{-1} stabilization of the transition state by the parent catalyst **Zn(OH$_2$)$_6$**.

The impressive 6.6 kcal mol^{-1} transition state stabilization by the minimal catalyst **Zn(OH$_2$)$_6$** in the polar solvent water is a dramatic illustration of the advantage for recruitment of metal dication(s) by enzyme catalysts of phosphate diester cleavage.[26–28] The interaction between **Zn(OH$_2$)$_6$** and the transition state includes electrostatic interaction as well as stabilization by covalent interactions between the oxygen electrons of the phosphorane-like transition state and orbitals of the zinc catalyst. In addition, the net stabilization of the transition state will depend upon the balance between the interaction of Zn(II) with water in competition with the dianionic transition state.

Ligand effects

The rate constants for **Zn(OH$_2$)$_6$**-catalyzed cleavage of **HpPNP** could only be determined at pH ≤ 7.4, because of the low solubility of free Zn(II). This illustrates that an important role of the ligand is to increase the solubility of the catalyst at high pH where there is a much higher concentration of the reactive form of the substrate **HpPNP$^-$** containing an ionized C-2 hydroxyl group.

Macrocycle affinity for Zn(OH$_2$)$_6$. The replacement of water molecules of **Zn(OH$_2$)$_6$** by three or four donor atoms of the macrocycles **1–4** does not cause a large change in the catalytic reactivity of the metal ion (Table 1). The failure to observe a large effect of Zn(II)-complex formation on reactivity does not mean that there are no such ligand effects. Rather, the small effect observed may result from the cancellation of larger opposing effects that cause an increase and decrease in the reactivity of **Zn(OH$_2$)$_6$**. For example, the formation of a tightly bound Zn(II) macrocyclic complex will shift positive charge from the metal cation to the macrocycle and cause a decrease in the reactivity of the metal cation as an electrophilic catalyst,[29–31] while the macrocyclic ligand may enforce a geometry at the Zn(II) center that leads to more favorable interactions with substrate/transition state. Note that the strong anion binding properties of **Zn(3)** have been attributed to a preference for the formation of four-coordinate complexes,[32] because a lowered coordination number leads to stronger ligand interactions.[27]

It is probably significant that the two macrocycle complexes that are the least reactive towards catalysis of **HpPNP** cleavage at low pH, **Zn(1)(OH$_2$)** and **Zn(4)(OH$_2$)**, show the largest values of K_{mac} for metal ion complex formation, while the two most reactive complexes, **Zn(2)(OH$_2$)** and **Zn(3)(OH$_2$)**, show the smallest values of K_{mac}. This trend provides evidence that the catalytic activity depends upon the strength of the interactions between Zn(II) and the macrocycle ligand. This may reflect a global effect of electron-donation from the ligand to metal cation on electrophilic reactivity as suggested above, or a specific requirement that the substrate have ready access to one of the coordination sites of the macrocycle.

Acidity of zinc-bound water. There is a significant variation in the values of $k_{zn}k_a/k_w$ for catalysis of the cleavage of **HpPNP** by **Zn(1)(OH$_2$)**, **Zn(2)(OH$_2$)** and **Zn(3)(OH$_2$)** which show nearly the same pK_a for deprotonation of Zn(II)-bound water. On the other hand, similar values of $k_{zn}k_a/k_w$ are observed for catalysis of **HpPNP** cleavage by **Zn(1)(OH$_2$)** and **Zn(4)(OH$_2$)** which both show substantially different pK_a values for the deprotonation of Zn(II)-bound water. We conclude that the pK_a is a not a good predictor of the catalytic activity of the **Zn(X)(OH$_2$)** studied in this work. The absence of a correlation may reflect the larger variation in the structure of macrocycles **Zn(1)–Zn(4)** than in earlier studies where a correlation between pK_a was observed.[33]

Binding affinity of monoanions and dianions

Each of the four **Zn(X)(OH$_2$)** catalysts studied in this work form complexes to phosphate and oxalate dianions with a much higher affinity than to diethyl phosphate monoanion (Table 2). Williams *et al.* have reported a large difference in the values of K_i = 10 mM and 5 μM for inhibition by diethyl phosphate monoanion and phenyl phosphate dianion, respectively, of **HpPNP** cleavage catalyzed by a highly reactive aqua form of a mononuclear Zn(II) complex,[4] and we have observed a large discrimination between the binding of methyl phosphate dianion and diethyl phosphate monoanion by **Zn$_2$(5)(OH$_2$)**.[23] These results support the proposal that these catalysts show selectivity for binding the transition state dianion compared with the reactant monoanion.

The observation that **3** shows the weakest affinity of the four macrocycles studied for binding to Zn^{2+} (Table 1), while **Zn(3)** shows the strongest affinity for binding to oxalate dianion and the second strongest affinity for binding to methyl phosphate dianion suggests that a strengthening of macrocycle–Zn^{2+} interactions has the effect of weakening the interactions with other bound ligands. However, we are unable to recognize any inclusive correlations between the relative kinetic parameters $k_{zn}k_a/k_w$ for **Zn(X)(OH$_2$)**-catalyzed cleavage of **HpPNP**, and the relative affinities of these different catalysts for binding of either methylphosphate or oxalate dianion The absolute dianion binding energies calculated from the kinetic parameters by substitution into eqn (5) of k_{HO} = 0.099 M^{-1} s^{-1} and $k_{zn}k_a/k_w$ from Table 1 gives a transition state stabilization of $\Delta G_{S\dagger}$ = 5.7, 7.4, 7.4 and 5.9 kcal mol^{-1} for **Zn(1)**, **Zn(2)**, **Zn(3)** or **Zn(4)**, respectively. The transition state binding energies and the ground state binding energies calculated from the inhibition constants reported in Table 2 are much larger than the *differences* in these binding energies for the four Zn(II) macrocyclic complexes. This suggests that all Zn(II) complexes bind tightly to dianionic ligands, but that the final complex stability depends in a complicated manner on the interaction of the dianionic ligand with the Zn(II) center. An important complicating factor is the highly variable coordination number of Zn(II) complexes. Certain Zn(II) catalysts bind simple anionic ligands with a concomitant increase in coordination number while other Zn(II) complexes do not.[34–36] Such differences in binding interactions will depend on the flexibility of the multidentate or macrocyclic ligands in accommodating different Zn(II) complex coordination numbers and geometries.

Conclusions

The macrocyclic ligands **1–4** serve primarily to keep Zn(II) in basic aqueous solution, where the model RNA substrate **HpPNP** shows a high reactivity towards catalyzed cleavage to form a cyclic phosphate and 4-nitrophenoxide ion. The effect of the interactions between the macrocycles **1–4** and Zn^{2+} is to cause either a modest enhancement, or loss, of catalytic activity. The observation that the best Zn^{2+}–macrocycle catalysts are those where the interactions between the metal ion and macrocycle are the weakest suggests that it might be useful to strive for good, but not exceptionally strong sets of donor groups in designing these catalysts. There are small variations in the magnitude of the stabilizing interactions between **Zn(X)(OH$_2$)** and either stable inhibitor dianions or the metastable dianionic transition state for cleavage of **HpPNP**. We are unable to provide a complete rationalization for these changes, and suggest that they are controlled by the poorly-defined details of the anion–catalyst interaction including the possible expansion[34, 35] of the Zn(II) coordination sphere upon ligand binding. The notion that **Zn(X)(OH$^-$)** complexes are not active catalysts suggests that improvement might be realized by incorporating functional groups that promote selective interactions with phosphate ester anions and decrease the strength of hydroxide binding.

Experimental

All reagents and solvents were of reagent grade and were used without further purification unless otherwise noted. The ligand **1** was purchased from Aldrich as the HBr salt. The ligand **3** was purchased as the free base from Strem chemicals. The ligands **2** and **4** as well as the RNA analog **HpPNP** were prepared by published procedures.[37–39] ^{1}H NMR spectra were recorded on a Varian Inova 500 spectrometer. All aqueous solutions were prepared using Millipore MILLI-Q purified water. Stock solutions (50.0 mM) of ligands in water were prepared from their respective salts, and the ligand concentrations were determined by ^{1}H NMR using *p*-toluene sulfonic acid as an internal standard. The concentration of solutions of $Zn(NO_3)_2$ were determined by titration with ethylenediaminetetraacetic acid (EDTA) using Eriochrome Black T as the indicator.[40]

Potentiometric titrations

Potentiometric titrations were conducted on a Brinkmann Metrohm 702 SM Titrino autotitrator using an Orion Research Ross combination pH electrode 8115BN. The Zn(II) complexes of the macrocycles were prepared in water by mixing $Zn(NO_3)_2$ and the corresponding HCl salt of the ligand in a 1 : 1.05 molar ratio. The concentrations of the macrocycle were determined by

^{1}H NMR spectroscopy as described above because the number of chlorides in the HCl salt of the macrocycle is unknown. The potentiometric titrations were carried out at $I = 0.10$ M ($NaNO_3$) and 25 °C. A minimum of two independent titrations were performed. Aqueous solutions (50 mL) that contain the Zn(II) macrocyclic complex were titrated using carbonate-free 0.10 M NaOH. The program HYPERQUAD 2000 Version 2.1 NT was used to obtain equilibrium constants by fitting the data and using a value of $K_w = ([H^+][OH^-]) = 10^{-13.79}$ determined for these experimental conditions. This least-squares refinement was carried out to obtain the best combination of acceptable values of the weighted error in the residuals σ^2 ($\sigma^2 \leq 9$ or $\sigma \leq 3$) and the goodness of fit statistic χ^2 at 95% confidence ($\chi^2 \leq 12.6$)

Transesterification of 2-hydroxypropyl 4-nitrophenyl phosphate (HpPNP)

The transesterification of **HpPNP** was monitored by following the increase in absorbance at 400 nm due to the release of 4-nitrophenolate. The following buffers were used in these experiments: 2-(*N*-morpholino)ethanesulfonic acid (MES, pH 6–6.5), *N*-(2-hydroxyethyl)piperazine-*N*′-(2-ethanesulfonic acid) (HEPES, pH 7.1–7.8), *N*-(2-hydroxyethyl)piperazine-*N*′-(3-propanesulfonic acid) (EPPS, pH 8.0–8.4), 2-(*N*-cyclohexylamino)ethanesulfonic acid (CHES, pH 8.9–9.3) and 3-(cyclohexylamino)-1-propanesulfonic acid (CAPS, pH 10–10.5). Zn(II) complexes of the macrocycles were prepared in water by mixing $Zn(NO_3)_2$ and the HCl salt of the ligand in a 1 : 1.05 molar ratio and adjusting the pH to 6.5 with NaOH. The solution of the metal complex was then mixed with buffer to give a final buffer concentration of 20 mM at $I = 0.10$ ($NaNO_3$) and adjusted to the desired pH. Cleavage reactions at 25 °C were initiated by injection of a solution of **HpPNP** to give a final concentration of 0.02 mM. Some rate constants were determined from the initial reaction, which required the use of a higher final concentration of 0.04 mM **HpPNP**. The pH of these solutions was determined at the end of each experiment, and found to be within 0.03 units of the initial value.

The concentrations of the catalysts were varied from 0.2–4.0 mM in experiments to determine second-order rate constants for reactions catalyzed by Zn(II)-complexes. Catalysis by $\mathbf{Zn(OH_2)_6}$ was studied over the following ranges of catalyst concentrations: pH 6.8, 2.0–5.0 mM, pH 7.0, 0.50–2.0 mM, pH 7.2, 1.0–2.5 mM, and, pH 7.4, 0.40–1.0 mM. In cases where the concentration of catalyst was ≥ 1 mM, the cleavage of **HpPNP** was monitored for > 3 half-lives and pseudo first-order rate constants, k_{obsd}, were determined as the slopes of the semilogarithmic plots of reaction progress against time. For reactions carried out in the presence of low concentrations of catalyst or high concentrations of inhibitor, the cleavage of **HpPNP** was monitored during the disappearance of the first 5–10% of the substrate. The temperature was then increased to 60 °C and maintained until the endpoint was reached. Values of k_{obsd} (s^{-1}) were determined as $k_{obsd} = v_i/[S]_o$, where v_i is the initial reaction velocity and $[S]_o$ is the initial substrate concentration determined from the total change in absorbance during the reaction. In all cases, standard deviations from the k_{obsd} values were <7%. Second-order rate constants (k_{Zn}) for the reactions catalyzed by hydrated Zn(II) and Zn(II) complexes were obtained as the slopes of linear plots of k_{obsd} (s^{-1}) against the catalyst concentration, for k_{obsd} determined in the presence of a minimum of five different concentrations of the catalyst ($r \geq 0.997$).

Acknowledgements

J. R. M. and J. P. R. thank the National Science Foundation (CHE-9986332) for their support of this work.

References

1 G. Feng, D. Natale, R. Prabaharan, J. C. Mareque-Rivas and N. Williams, *Angew. Chem., Int. Ed. Engl.*, 2006, **45**, 7056–7059.
2 T. Lonnberg and H. Lonnberg, *Curr. Opin. Chem. Biol.*, 2005, **9**, 665–673.
3 O. Iranzo, A. Y. Kovalevsky, J. R. Morrow and J. P. Richard, *J. Am. Chem. Soc.*, 2003, **125**, 1988–1993.
4 G. M.-R. Feng, J. C. Martin de Rosales and R. T. N. H. Williams, *J. Am. Chem. Soc.*, 2005, **127**, 13470–13471.
5 M. Yashiro, H. Kaneiwa, K. Onaka and M. Komiyama, *J. Chem. Soc., Dalton Trans.*, 2004, 605–610.
6 J. R. Morrow and O. Iranzo, *Curr. Opin. Chem. Biol.*, 2004, **8**, 192–200.
7 G. Feng, J. C. Mareque-Rivas and N. Williams, *Chem. Commun.*, 2006, 1845–1847.
8 M.-Y. Yang, J. P. Richard and J. R. Morrow, *Chem. Commun.*, 2003, **22**, 2832–2833.
9 O. Iranzo, T. Elmer, J. P. Richard and J. R. Morrow, *Inorg. Chem.*, 2003, **42**, 7737–7746.
10 M.-Y. Yang, O. Iranzo, J. P. Richard and J. R. Morrow, *J. Am. Chem. Soc.*, 2005, **127**, 1064–1065.
11 A. M. O'Donoghue, S. Y. Pyun, M.-Y. Yang, J. R. Morrow and J. P. Richard, *J. Am. Chem. Soc.*, 2006, **8**, 1615–1621.
12 V. M. Shelton and J. R. Morrow, *Inorg. Chem.*, 1991, **30**, 4295–4299.
13 T. Kioke and E. Kimura, *J. Am. Chem. Soc.*, 1991, **113**, 8935–8941.
14 V. J. Thom, M. S. Shaikjee and R. D. Hancock, *Inorg. Chem.*, 1986, **25**, 2992–3000.
15 A. Bencini, E. Berni, A. Bianchi, C. Giorgi and B. Valtancoli, *Supramol. Chem.*, 2001, **13**, 489–497.
16 J. R. Morrow, L. A. Buttrey and K. A. Berback, *Inorg. Chem.*, 1992, **31**, 16–20.
17 R. Breslow, D. Huang and E. Anslyn, *Proc. Natl. Acad. Sci. USA*, 1989, **86**, 1746–1750.
18 J. Burgess, *Metal Ions in Solution*, Ellis Horwood Limited, New York, 1978.
19 A. E. Martell, *Critical Stability Constants*, Plenum Press, New York, 1974.
20 H. Lonnberg, R. Stromberg and A. Williams, *Org. Biomol. Chem.*, 2004, **2**, 2165–2167.
21 C. F. J. Base, R. E. Mesmer, *The Hydrolysis of Cations*, John Wiley & Sons, New York, 1976.
22 L. J. Zompa, *Inorg. Chem.*, 1978, **17**, 2531–2536.
23 M.-Y. Yang, J. R. Morrow and J. P. Richard, *Bioorg. Chem*, 2007, DOI: 10.1016/j.bioorg.2007.02.003.
24 R. Wolfenden and M. J. Snider, *Acc. Chem. Res.*, 2001, **34**, 938–945.
25 A. K. Yatsimirsky, *Coord. Chem. Rev.*, 2005, **249**, 1997–2011.
26 E. Kimura, *Curr. Opin. Chem. Biol.*, 2000, **4**, 207–213.
27 I. Bertini, C. Luchinat, M. Rosi, A. Sgamellotti and F. Tarantelli, *Inorg. Chem.*, 1990, **29**.
28 D. E. Wilcox, *Chem. Rev.*, 1996, **96**, 2435–2458.
29 Y.-H. Chiu and J. W. Canary, *Inorg. Chem.*, 2003, **42**, 5107–5116.
30 J. W. Canary, J. Xu, J. M. Castagnetto, D. Rentzeperis and L. A. Marky, *J. Am. Chem. Soc.*, 1995, **117**, 11545–11547.
31 J. W. Canary, G. J. Gabriel and Y.-H. Chiu, *Inorg. Chem.*, 2005, **44**, 40–44.
32 E. Kimura, T. Shiota, T. Koike, M. Shiro and M. Kodama, *J. Am. Chem. Soc.*, 1990, **112**, 5805–5811.
33 L. Bonfa, M. Gatos, F. Mancin, P. Tecilla and U. Tonellato, *Inorg. Chem.*, 2003, **42**, 3943–3949.

34 M. Rombach, C. Maurer, K. Weis, E. Keller and H. Vahrenkamp, *Chem. Eur. J.*, 1999, **5**, 1013–1027.
35 H. Vahrenkamp, *Acc. Chem. Res.*, 1999, **32**, 589–596.
36 T. Tekeste and H. Vahrenkamp, *Eur. J. Inorg. Chem.*, 2006, 5158–5164.
37 C. S. Rossiter, R. A. Mathews and J. R. Morrow, *Inorg. Chem.*, 2005, **44**, 9397–9404.
38 K. P. McCue, University at Buffalo, PhD thesis, University at Buffalo, State University of New York, 1999.
39 D. M. Brown and D. A. Usher, *J. Am. Chem. Soc.*, 1965, 6558–6564.
40 J. Basset, R. C. Denney, G. H. Jeffery and J. Mendham, *Titrimetric Analysis. Vogel's Textbook of Quantitative Inorganic Analysis*, John Wiley & Sons, New York, 1978.